Stem Cell Research (2011) 7, 244–255

available at www.sciencedirect.com

www.elsevier.com/locate/scr

REGULAR ARTICLES

Dual stem cell therapy after myocardial infarction acts specifically by enhanced homing via the SDF-1/CXCR4 axis

Hans D. Theiss [a, 1], Markus Vallaster [a, 1], Christoph Rischpler [a, 1], Lisa Krieg [a], Marc-Michael Zaruba [a], Stefan Brunner [a], Yordan Vanchev [a], Rebekka Fischer [a], Michael Gröbner [a], Bruno Huber [a], Timm Wollenweber [c], Gerald Assmann [b], Josef Mueller-Hoecker [b], Markus Hacker [c], Wolfgang-M. Franz [a,*]

[a] *Medical Department I, Klinikum Grosshadern, Ludwig-Maximilians-University, Munich, Germany*
[b] *Institute of Pathology, Ludwig-Maximilians-University, Munich, Germany*
[c] *Department of Nuclear Medicine, Klinikum Grosshadern, Ludwig-Maximilians-University, Munich, Germany*

Received 29 October 2010; received in revised form 22 April 2011; accepted 8 May 2011
Available online 16 May 2011

Abstract *Background:* G-CSF based stem cell mobilization and stabilization of cardiac SDF-1 by DPP-IV-inhibition (dual stem cell therapy) improve heart function and survival after myocardial infarction. However, it is barely understood whether this new approach acts specifically through the SDF-1/CXCR4 axis, stimulation of resident cardiac stem cells and improved myocardial perfusion. Therefore, we aimed to clarify the role of the SDF1/CXCR4 axis with respect to the benefits of a dual stem cell based therapy.

Methodology/principal findings: After surgically induced ligation of the LAD, SDF-1/CXCR4 interactions were specifically blocked by the CXCR4 receptor antagonist AMD3100 in G-CSF and Diprotin A treated C57BL/6 mice. G-CSF + DipA treated and non-treated animals served as controls. Because AMD3100 is known to mobilize bone marrow derived stem cells (BMCs) in high concentrations, the optimal dosage (1.25 mg per kg body weight) sufficient to block CXCR4 without stimulating mobilization was established. AMD3100 treatment of G-CSF and Diprotin A stimulated mice significantly decreased myocardial homing of circulating stem cells (FACS analysis) and inverted the beneficial effects of (i) cardiac remodeling (histological analyses), (ii) heart function (Millar tip catheterization) and (iii) survival (Kaplan–Meier curves). G-CSF treatment in combination with DPP-IV inhibition enhanced neovascularization at the infarct border zone which was related to an improved myocardial blood flow as measured by SPECT. Moreover, dual stem cell treatment effectively stimulated the pool of resident cardiac stem cells (FACS) which was reversed by AMD3100 treatment.

Conclusions/significance: Our data give final proof that homing through the SDF-1/CXCR-4 axis is essential for the success of dual stem cell therapy.

* Corresponding author at: Ludwig Maximilians University, Medical Department I — Cardiology, Klinikum Grosshadern, Marchioninistr. 15, 81377 Munich, Germany. Fax: +49 89 7095 6094.
E-mail address: wolfgang.franz@med.uni-muenchen.de (W.-M. Franz).
[1] Authors contributed equally to this work.

1873-5061/$ - see front matter © 2011 Elsevier B.V. All rights reserved.
doi:10.1016/j.scr.2011.05.003

Introduction

In industrial nations, ischemic disorders in general are the main cause of death in human beings (Dickstein et al., 2008). After myocardial infarction, damages of cardiac tissue are irreversible and lead to progressive ischemic cardiomyopathy. However, stem cell mobilization and migration into the heart could be a new therapeutic approach to improve myocardial function and survival after ischemic injury since they stimulate neovascularization and prevent apoptosis of cardiomyocytes by paracrine means (Balsam et al., 2004; Fazel et al., 2006; Murry et al., 2004; Zaruba et al., 2008). While experiments using granulocyte-colony stimulating factor (G-CSF) based stem cell mobilization in mice showed great promise (Deindl et al., 2006; Orlic et al., 2001), only few human trials reported an improvement of cardiac function (Ince et al., 2005a; Ince et al., 2005b), whereas most of them could not demonstrate beneficial effects (Engelmann et al., 2006; Engelmann et al., 2010; Zohlnhofer et al., 2008).

Recently, we advanced the approach of therapeutic stem cell mobilization by contemporaneous enhancement of cardiac homing capacity (Zaruba et al., 2009). Although homing of circulating stem cells is mediated by several parameters like stem cell factor (SCF) or hepatocyte growth factor (HGF), the interaction of CXCR4 and myocardial stromal cell-derived factor (SDF-1) appeared to be the most relevant axis (Abbott et al., 2004; Aiuti et al., 1997; Askari et al., 2003; Ceradini et al., 2004; Franz et al., 2003; Saxena et al., 2008; Segers et al., 2007). SDF-1 binds to CXCR-4 in its active form (1–68) (Crump et al., 1997) and is cleaved N-terminally at its position-2 proline by CD26/dipeptidylpeptidase IV (DPP-IV), which is a membrane-bound extracellular peptidase (Christopherson et al., 2004) that is ubiquitously expressed (Huhn et al., 2000; Kahne et al., 1999; Ruiz et al., 1998; Vanham et al., 1993). Combining genetic or pharmacological inhibition of CD26/DPP-IV with G-CSF based stem cell mobilization, we could demonstrate stabilization of myocardial SDF-1, enhanced cardiac recruitment of bone marrow-derived stem cells, improved myocardial function and increased survival in the mouse model (Zaruba et al., 2009). Thereupon, we transferred this new approach from bench to bedside and initiated the first study (SITAGRAMI-Trial) analyzing dual stem cell therapy in patients suffering from acute myocardial infarction (Theiss et al., 2010).

However, we aimed to collect further evidence that the beneficial effects of this innovative dual therapeutic concept are specifically due to cardiac homing of bone-marrow derived stem cells via the SDF-1/CXCR4 axis since G-CSF and/or DPP-IV inhibition may exert direct effects on ischemic myocardium as well. Therefore, we antagonized specifically the CXCR4 receptor using AMD3100 after ligation of the left anterior descending artery (LAD) in mice and analyzed stem cell homing, infarct size, cardiac function and survival. Additionally, we analyzed the effect of a dual stem cell therapy on capillary formation and myocardial perfusion using SPECT technology. Finally, we intended to elucidate the role of resident cardiac stem cells after DPP-IV inhibition and G-CSF application. We hypothesized that the increased homing of bone-marrow derived stem cells also leads to a paracrine stimulation of resident cardiac stem cells, which also may contribute to the improvement of heart function and survival.

Results

Dose–response titration of AMD3100 with respect to stem cell mobilization

First, we aimed to establish the optimal dosage of AMD3100 that is sufficient to block CXCR4 without stimulating the mobilization of stem cells to a relevant extent (Broxmeyer et al., 2005). AMD3100 concentrations of 0.5, 1.25 and 5.0 mg/kg/d were administered and analyzed for the amount of $CD34^+/CD45^+$ and $CD34^+/CD45^+/CXCR4^+$ stem cells in the peripheral blood at day 2 after MI (Fig. 1).

Using AMD3100 concentrations of 0.5 and 1.25 mg/kg/d, we detected no relevant mobilization of $CD34^+/CD45^+/CXCR\text{-}4^+$ progenitor cells and only slight mobilization of $CD34^+/CD45^+$ cells (using 1.25 mg/kg/d). In contrast, application of 5.0 mg/kg AMD3100 leads to a 10-fold increase of circulating $CD34^+/CD45^+$ and $CD34^+/CD45^+/CXCR\text{-}4^+$ stem cells. On this basis, we used AMD3100 at the concentration of 1.25 mg/kg/d for further experiments.

AMD3100 antagonizes the benefit of DPP-IV inhibition on cardiac SC homing

Second, we analyzed the impact of AMD3100 administration on the myocardial homing of bone marrow derived stem cells. As shown in Fig. 2, application of G-CSF and Diprotin A significantly increased the numbers of bone-marrow derived $CD34^+/CD45^+$, $CD34^+/CD45^+/CXCR4^+$ as well as $lin^-/Sca\text{-}1^+/c\text{-}kit^+$ stem cell populations in the heart not only at day 2 (as shown previously) (Zaruba et al., 2009) but also even at day 6 after MI (Fig. 2). This effect was significantly inverted by AMD3100 based CXCR4 antagonization. The relative numbers of $CD34^+/CD45^+$ ($1.32 \pm 0.31\%$ vs. $4.94 \pm 1.19\%$, $p<0.05$), $CD34^+/CD45^+/CXCR\text{-}4^+$ ($0.95 \pm 0.31\%$ vs. $4.16 \pm 1.06\%$, $p<0.05$) and $lin^-/Sca\text{-}1^+/c\text{-}kit^+$ (0.17 ± 0.03 vs. 0.66 ± 0.21, $p<0.05$) stem cells were significantly decreased in the [AMI + G-CSF + DipA + AMD] group compared to [AMI + G-CSF + DipA] animals suggesting specific inhibition of the SDF1–CXCR4-axis. Sole AMD3100 administration did not lead to significant effects in comparison to the saline group.

CXCR4 antagonism increased the size of infarction and led to pronounced wall thinning

Next, we investigated the effect of a CXCR4 antagonism with respect to LV remodeling after MI. In [AMI + G-CSF + DipA] animals, the size of infarction was significantly reduced 30 days after MI in comparison to the control group (Fig. 3). As shown in Fig. 3A, blocking of CXCR4 by AMD3100 significantly increased the size of infarction in the [AMI + G-CSF + DipA + AMD] group compared to [AMI + G-CSF + DipA] ($32.3 \pm 4.1\%$ vs. $23.4 \pm 1.5\%$, $p<0.05$). In parallel, histological analyses revealed a significant LV wall thinning in [AMI + G-CSF + DipA + AMD] treated mice as compared to the [AMI + G-CSF + DipA] group at day 30 after MI (0.43 ± 0.01 mm vs. 0.22 ± 0.03 mm, $p<0.05$). Interestingly, the [AMI + G-CSF + DipA + AMD] group revealed similar values with respect to the infarct size and the LV wall thickness as G-CSF mono treated animals, suggesting that the additional benefits on cardiac remodeling are mainly due to stabilization of the SDF-1/CXCR4 axis by DPP-IV inhibition.

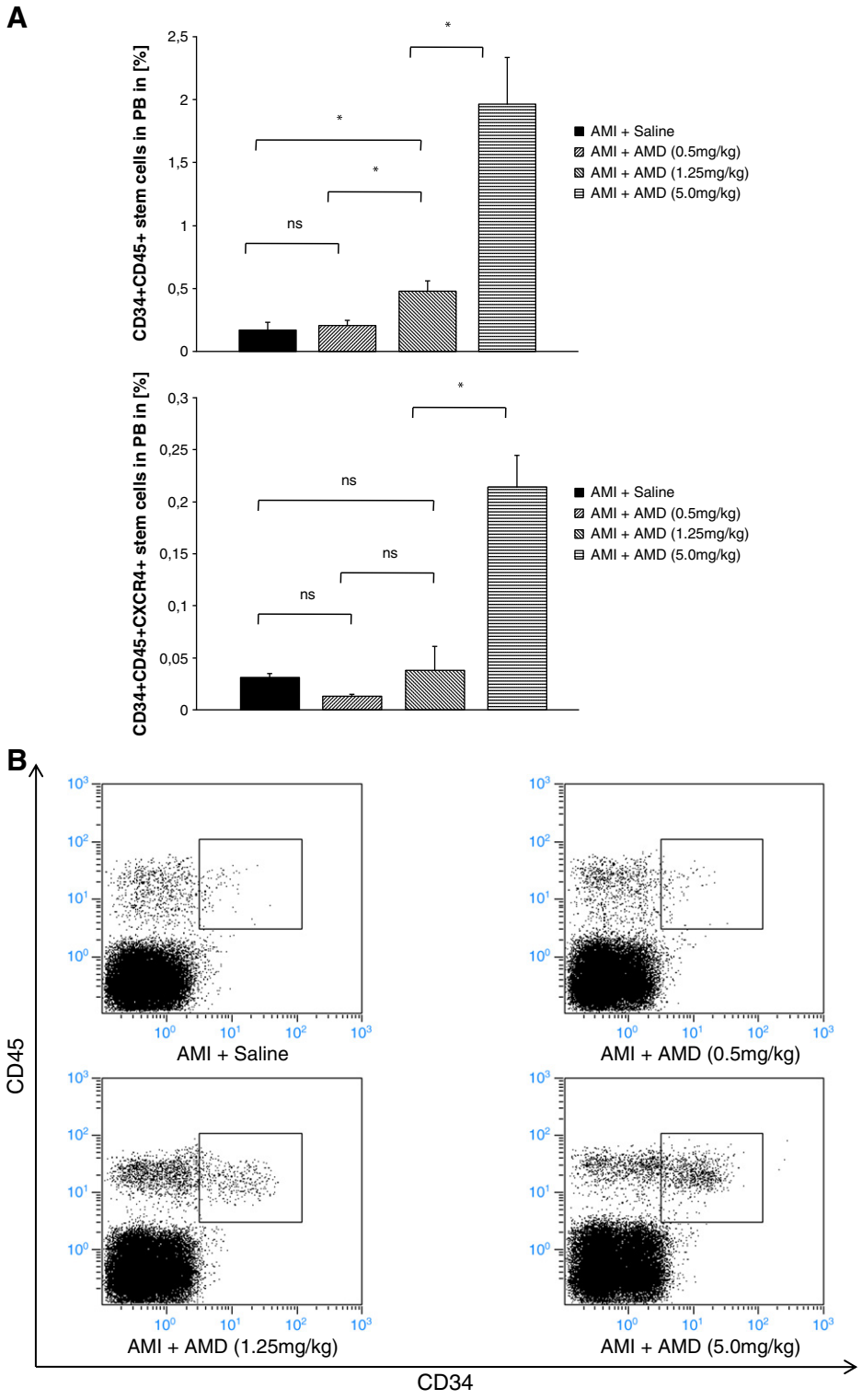

Figure 1 Dose–response titration of AMD3100 concerning stem cell mobilization. (A) Diagrams show the amount of bone marrow derived $CD34^+/CD45^+$ (upper row) and $CD34^+/CD45^+/CXCR\text{-}4^+$ (lower row) stem cells in different concentrations of AMD3100 (0.5, 1.25 and 5.0 mg/kg) and in controls in the peripheral blood 2 days after myocardial infarction. Data represent mean ± SEM (n = 6); [*] = $p<0.05$; [ns] = not significant. (B) Representative FACS plots showing the mean numbers of $CD34^+/CD45^+$ cells in the peripheral blood of mice treated with saline or AMD3100 in different concentrations (0.5, 1.25 and 5.0 mg/kg).

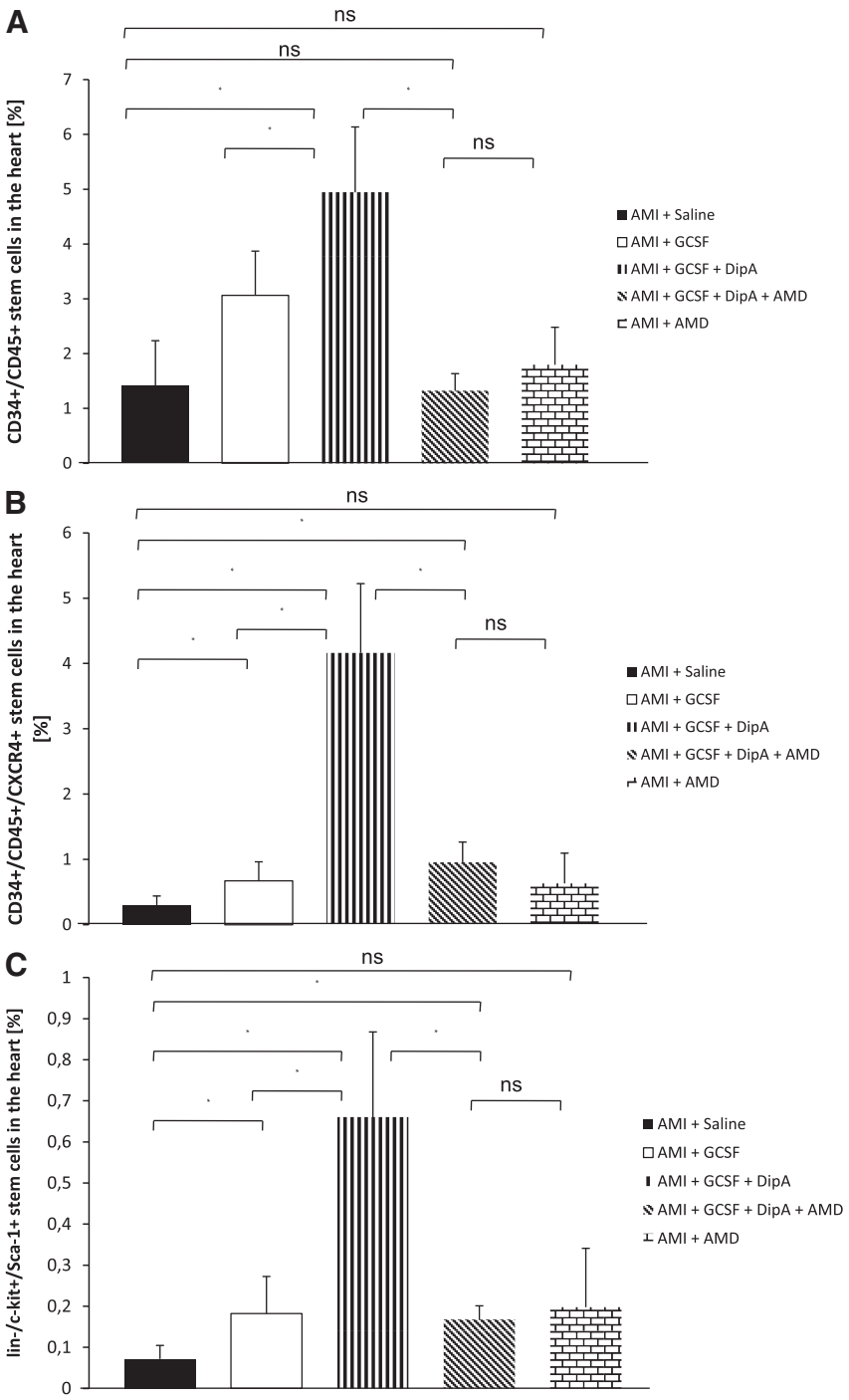

Figure 2 CXCR4 antagonization reverses cardiac SC homing in G-CSF + DipA treated mice. Histograms representing the percentage of myocardial $CD34^+/CD45^+$ (A), $CD34^+/CD45^+/CXCR\text{-}4^+$ (B) as well as $lin^-/c\text{-}kit^+/Sca\text{-}1^+$ (C) bone marrow derived stem cells 6 days after myocardial infarction. Data represent mean ± SEM (n = 8); [*] = $p < 0.05$; [ns] = not significant.

Blockage of SDF-1/CXCR-4 inverts the improvement of cardiac function

Having shown that CXCR4 antagonism impaired LV remodeling, we next evaluated the impact of AMD3100 treatment on cardiac function. Using conductance catheters, pressure volume relations were measured from [AMI + saline], [AMI + G-CSF], [AMI + G-CSF + DipA] and [AMI + G-CSF + DipA + AMD] groups (each n = 10) at day 30 after MI (Figs. 4A and B). Administration of AMD3100 inverted the improvement of ejection fraction in the [AMI + G-CSF + DipA] group (23.3 ± 2.6% vs. 35.0 ± 3.3%, $p < 0.05$). As another control group, sole administration of AMD3100 did not influence cardiac function significantly.

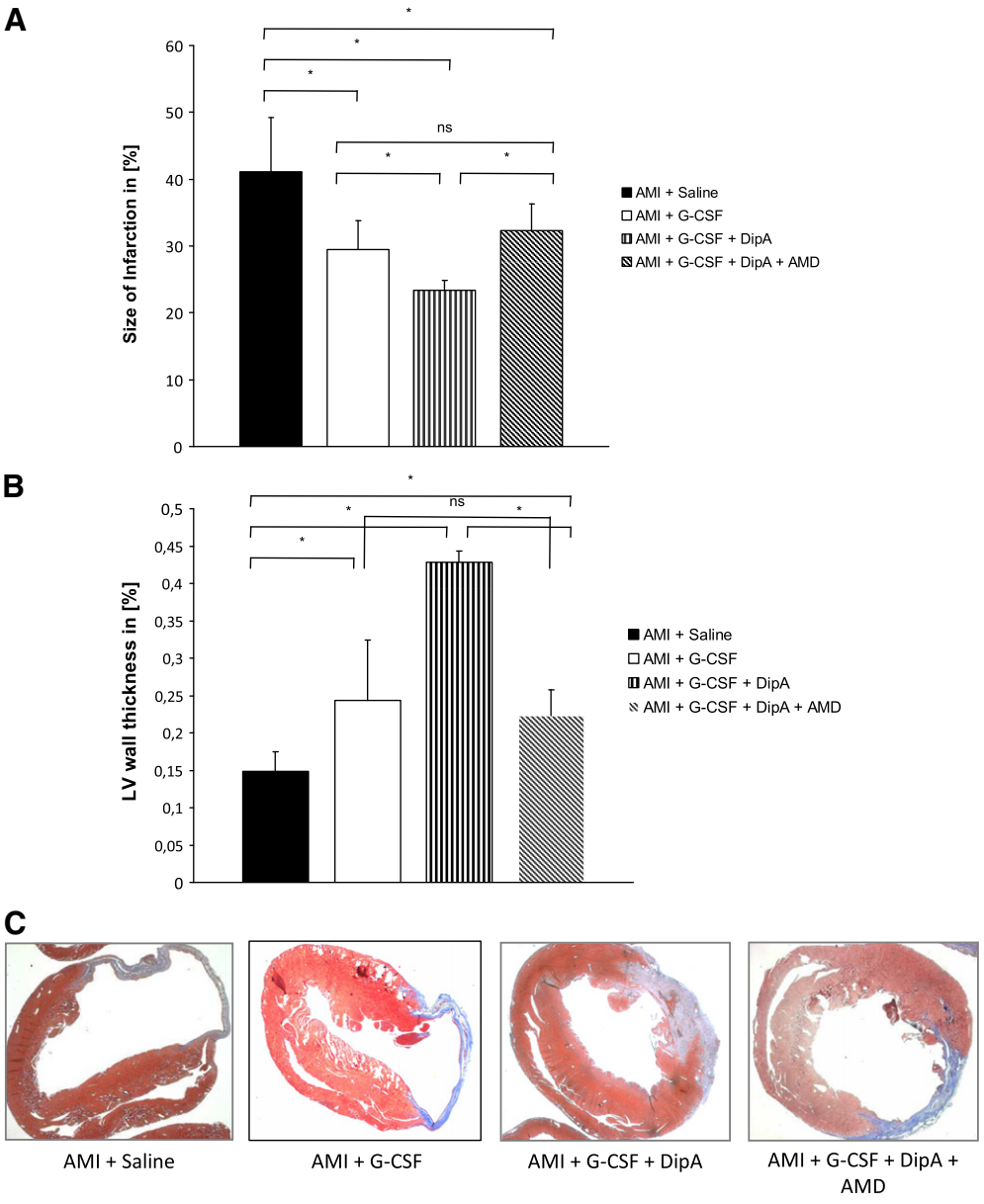

Figure 3 Effect of AMD3100 on the size of myocardial infarction and LV wall thickness. (A) and (B) Bar graphs representing the size of myocardial infarction as well as the thickness of the LV wall 30 days after myocardial infarction. Data represent mean ± SEM (n = 8); [*] = $p < 0.05$; [ns] = not significant. (C) Representative histological Masson's trichrome stainings of transverse heart sections in infarcted hearts 30 days after myocardial infarction.

In analogy, contractility and effective arterial elastance were declined in the [AMI + G-CSF + DipA + AMD] group. Diastolic heart function reflected by the isovolumetric relaxation parameter Tau weiss was also impaired (Suppl. 2). Thus, [AMI + G-CSF + DipA + AMD] mice showed a significantly decreased systolic and diastolic function in comparison to the [AMI + G-CSF + DipA] group.

AMD3100 application reverts advantage of survival

Cumulative survival of saline, G-CSF, G-CSF + DipA and G-CSF + DipA + AMD3100 treated mice (each with n = 23) was recorded for 30 days after ligation of LAD (Fig. 4C). Mortality was very high within the first 6 days after MI. The high early post-MI mortality is mainly due to ruptures of the left ventricle wall or cardiac arrhythmias. The [AMI + G-CSF + DipA] group showed highly increased survival rates (69.6%) in comparison to the saline treated group (34.8%). Notably, this effect was completely reversed by application of the CXCR-4 antagonist AMD3100. Only 39.1% of [AMI + G-CSF + DipA + AMD] mice were alive 30 days after MI, which is comparable to the G-CSF monotherapy.

Blockage of SDF-1/CXCR-4 axis reduces cardiac neovascularization

Since $CD34^+/CD45^+$ cells are known carriers of growth factors, we next evaluated the amount of neovascularization

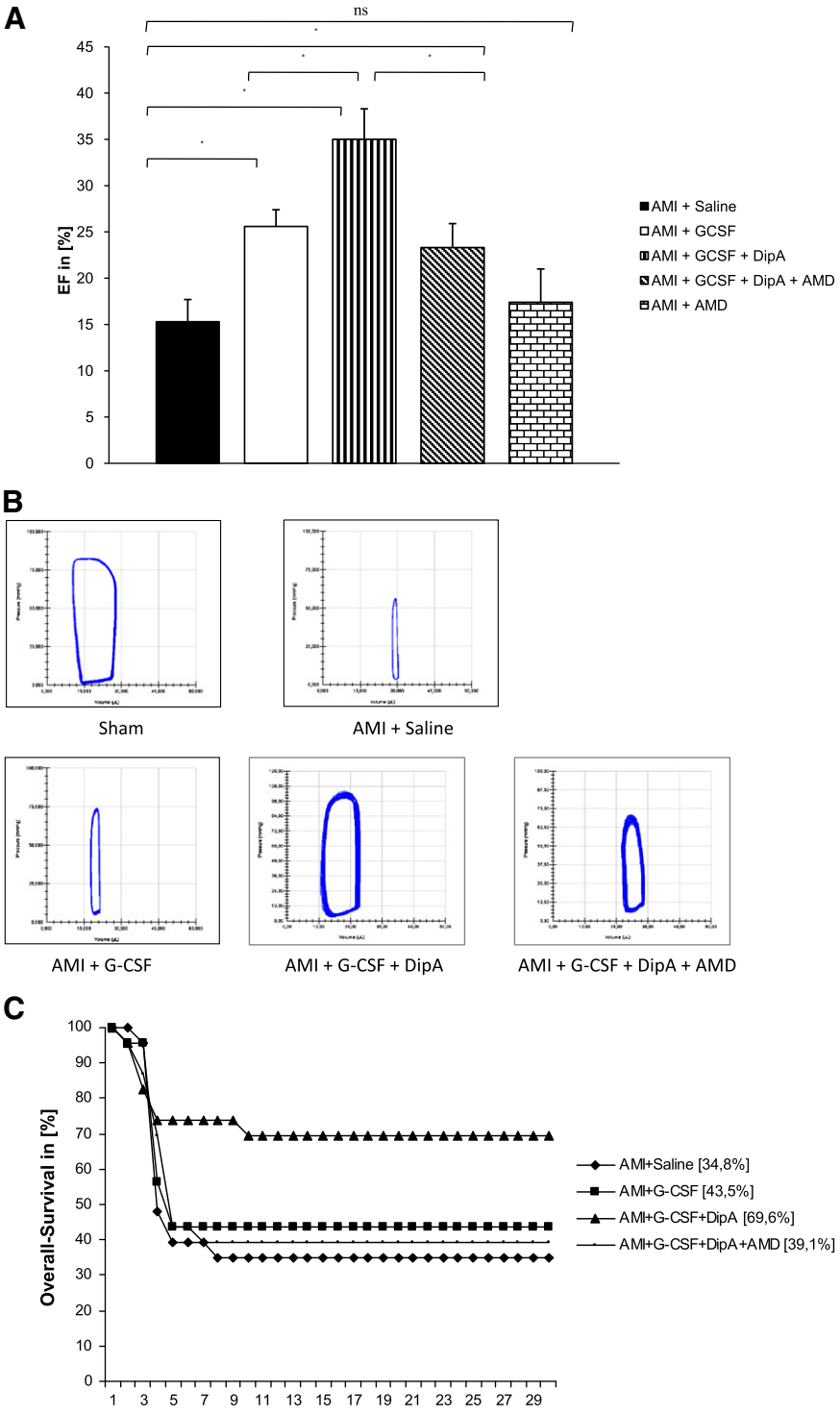

Figure 4 Analysis of cardiac function and survival after AMD3100 administration. (A) Bar graph representing the ejection fraction (EF) of [AMI + saline], [AMI + G-CSF], [AMI + G-CSF + DipA], [AMI + G-CSF + DipA + AMD] and [AMI + AMD] treated mice after ligation of LAD at day 30. Data represent mean ± SEM; n = 10; [*] = $p < 0.05$; [ns] = not significant. (B) Representative pressure volume loops of the aforementioned groups 30 days after myocardial infarction. (C) Kaplan–Meier curves showing survival rates of [AMI + saline], [AMI + G-CSF], [AMI + G-CSF + DipA] and [AMI + G-CSF + DipA + AMD] mice 30 days after acute myocardial infarction. All mice (n = 23 each group) revealed histologically confirmed myocardial infarctions.

and perfusion in the infarcted heart. G-CSF treatment and application of Diprotin A lead to significantly increased numbers of CD31 positive capillaries in the border zone as compared to non-treated animals or [AMI + G-CSF] mice (Fig. 5). The effect on neovascularization was reversed when CXCR4 was antagonized by AMD3100.

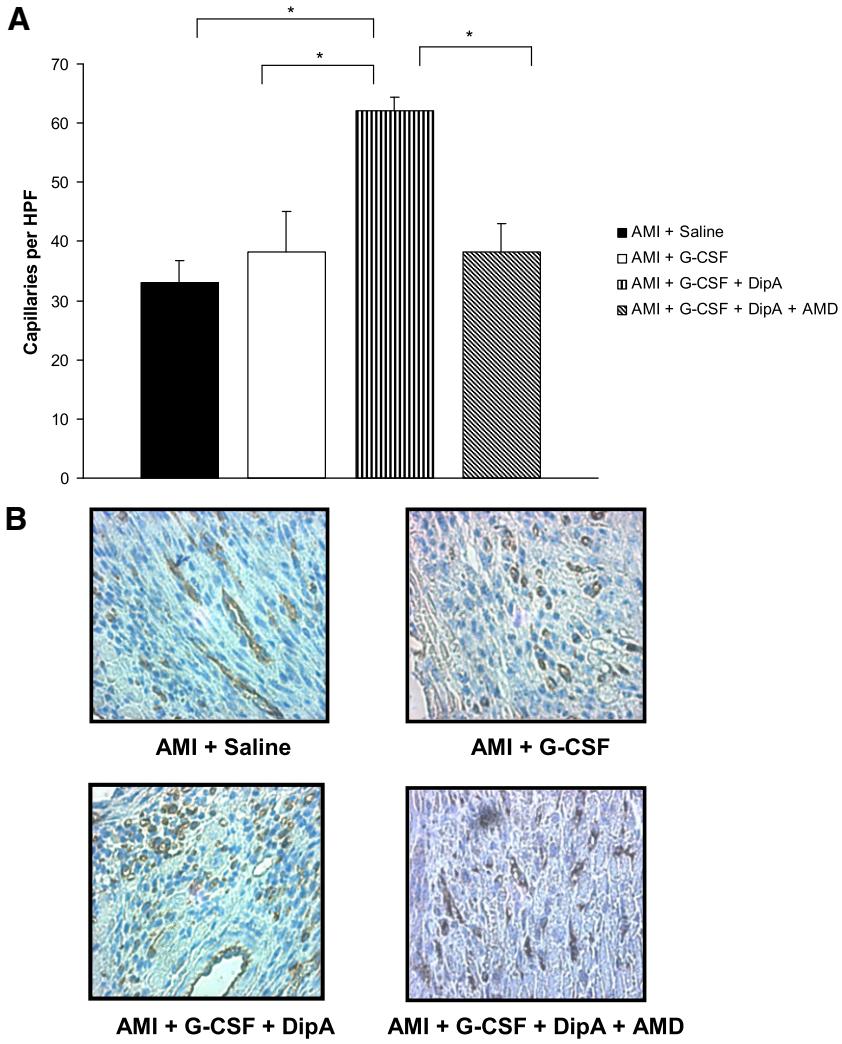

Figure 5 G-CSF and Diprotin A treatment enhance neovascularization. (A) Histogram shows that the numbers of $CD31^+$ capillaries in the infarct border zone is increased in [AMI + G-CSF + DipA] animals compared to [AMI], [AMI + G-CSF] and [AMI + G-CSF + DipA + AMD] mice. [*] = $p < 0.05$ (B) Representative immunohistochemical staining of CD31-positive capillaries (brown) in infarcted hearts 6 days after myocardial infarction.

Additionally, myocardial perfusion was repetitively and longitudinally analyzed by a clinical SPECT system equipped with pinhole collimators (Wollenweber et al., 2010). As shown in Fig. 6, myocardial perfusion exclusively decreased in the [AMI] group 30 days after MI (Fig. 6). In contrast, myocardial perfusion was markedly increased in [AMI + G-CSF + DipA] mice compared to both [AMI + G-CSF] and [AMI + G-CSF + DipA + AMD] mice. The decrease of myocardial perfusion in mice treated with the CXCR4 inhibitor AMD3100 suggests that the effects of dual stem cell therapy on myocardial perfusion are also dependent on an intact SDF1/CXCR4 axis.

Dual stem cell therapy stimulates $CD34^-/CD45^-/c\text{-}kit^+$ and $CD34^-/CD45^-/Sca1^+$ cells

G-CSF based stem cell mobilization combined with DPP-IV inhibition leads to a highly significant increase of so called resident cardiac stem cells (RCSC) defined as a population of $CD34^-/CD45^-/c\text{-}kit^+$ cells or $CD34^-/CD45^-/Sca1^+$ cells (Fig. 7). In comparison, after administration of AMD3100 only moderate enhancement of these cells was detected in the [AMI + G-CSF + DipA + AMD] group, which was in the same range as in [AMI + G-CSF] animals. Sole administration of AMD showed no relevant effect on RCSC (Fig. 8).

Discussion

Recently, we established the new therapeutic concept of a dual stem cell therapy after acute myocardial infarction which combines G-CSF induced stem cell mobilization and pharmacological SDF-1 stabilization by DPP-IV inhibition (Zaruba et al., 2009). However, the precise mechanisms of SDF-1/CXCR4 mediated cardiac repair are still barely understood. Therefore, we aimed to elucidate three important questions which remained open: 1. Were the effects of dual stem cell therapy on cardiac function and survival specifically exerted via the SDF1/CXCR4 axis? 2. Which role do neovascularization and myocardial perfusion play in

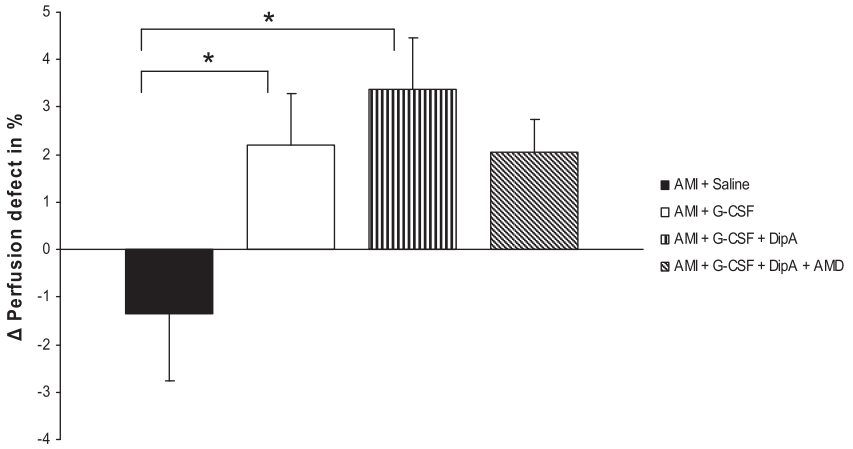

Figure 6 Dual stem cell therapy improves myocardial perfusion. Myocardial perfusion is enhanced in [AMI + G-CSF + DipA] mice compared to the other groups 30 days after myocardial infarction (assessed by gated single photon emission computed tomography (SPECT)). [*] = $p < 0.05$.

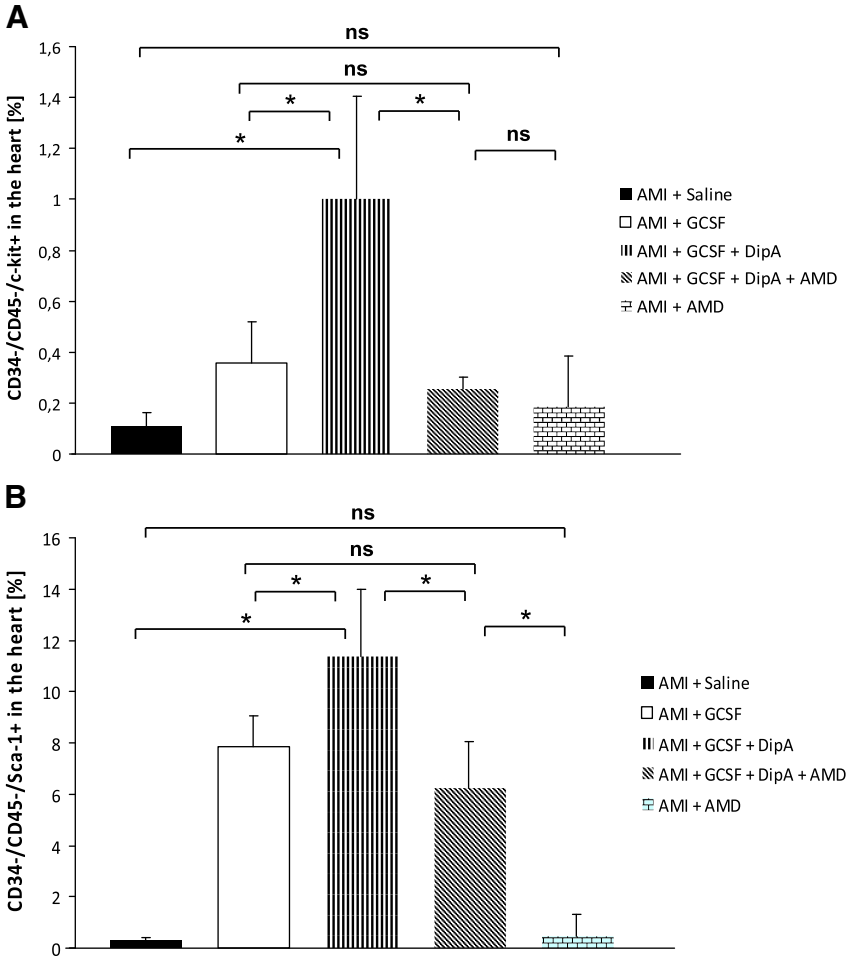

Figure 7 Dual stem cell therapy stimulates resident cardiac stem cells. Resident cardiac stem cells are defined as a populations of $CD34^-/CD45^-/c\text{-}kit^+$ and $CD34^-/CD45^-/Sca1^+$ cells. The diagram shows that G-CSF + DipA treatment leads to a significant increase of resident cardiac stem cells in comparison to the [AMI + saline] group (n = 8). This effect can be inverted by AMD administration.

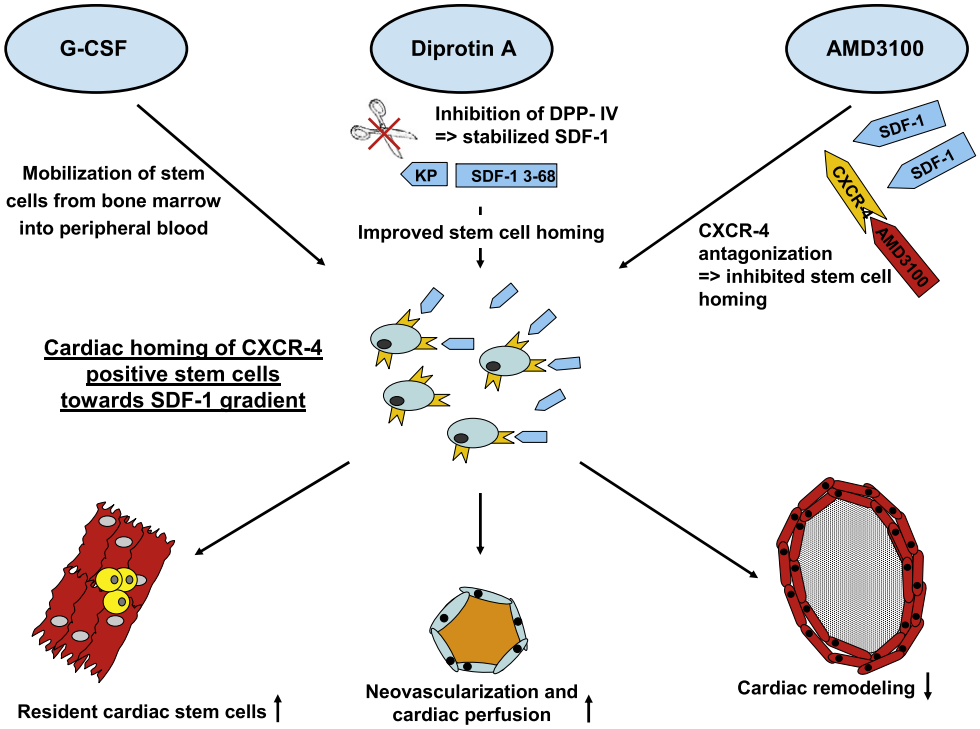

Figure 8 Schematic overview of SDF-1/CXCR4 mediated cardiac repair. Dual stem cell therapy works by two basic mechanisms. Application of G-CSF leads to stem cell mobilization from bone marrow into peripheral blood. DPP-IV inhibition (using Diprotin A) stabilizes myocardial SDF-1 thereby improving the cardiac homing of mobilized stem cells. After homing, mobilized stem cells stimulate resident cardiac stem cells, enhance myocardial perfusion and reduce cardiac remodeling. All these effects lead in addition to improved cardiac function and survival after myocardial infarction. This can be inverted by application of the CXCR4-antagonist AMD3100, which shows the dependence of a dual stem cell therapy on an intact SDF-1/CXCR4-axis.

CXCR4 mediated repair? 3. Does dual stem cell therapy affect the pool of resident cardiac stem cells?

Dual stem cell therapy works specifically by the SDF1—CXCR4-axis

In the current study, we applied the CXCR4 antagonist AMD3100 to specifically block CXCR4 mediated interactions. In other studies, AMD3100 was used for mobilizing stem cells from the bone marrow into peripheral blood (Broxmeyer et al., 2005). However, in these experiments AMD3100 was used at high concentrations of 5 mg/kg. In order to minimize the effects of AMD3100 on stem cell mobilization, we performed dose–response experiments to establish the highest possible dosage of AMD3100 that has negligible effects on stem cell mobilization. In our hands, an AMD3100 applied at a dosage of 1.25 mg/kg/d revealed low mobilizing activity and seemed sufficient for effective CXCR-4 antagonization. On this basis, we used AMD3100 at a concentration of 1.25 mg/kg to specifically block CXCR4 in our experiments.

Application of AMD3100 leads to reduced myocardial homing of circulating stem cells, impaired post-MI remodeling and deterioration of cardiac function as well as survival. These data suggest that the combined application of G-CSF and Diprotin A mainly works through an intact SDF1/CXCR4 axis although other factors like HGF or SCF also contribute to the homing process. Our results further underline the importance of combining G-CSF and DPP-IV inhibition. Apparently, the extent of stem cell homing is decisive for the success of our therapeutic approach although other direct cardiac effects of G-CSF (Harada et al., 2005) and Diprotin A also may exist.

Myocardial perfusion is enhanced by dual stem cell therapy

Another crucial question is to which extent different mechanisms contribute to the success of dual stem cell therapy. One essential factor is myocardial perfusion since rescued cardiomyocytes and resident cardiac stem cells definitively need enough blood supply to regenerate the infarcted myocardium. First, we showed that the increase of CD31 positive capillaries induced by dual stem cell therapy in the border zone could be reversed by CXCR4 antagonization suggesting that the effects on neovascularization are specifically mediated through an intact SDF-1/CXCR4 axis. Secondly, we analyzed myocardial perfusion by SPECT analysis, which is very compelling because measurements can be performed at several time points in the same animal. Our group has previously shown that SPECT analysis is applicable for perfusion studies after myocardial infarction (Wollenweber et al., 2010). Using this method, we now examined the time course of cardiac blood flow over 30 days after myocardial infarction under G-CSF therapy and DPP-IV-inhibition. Notably, dual stem cell therapy enhanced myocardial perfusion after 30 days in comparison to non-treated animals or mice receiving G-CSF-monotherapy. These results are very important since the combination of improved blood flow in

the (peri) infarct zone and regeneration of myocardium seems to be crucial for true repair of infarcted hearts.

Dual stem cell therapy stimulates "resident cardiac stem cells"

Finally, we analyzed the impact of this new therapeutic approach on so called resident cardiac stem cells (RCSC). Using the combination of G-CSF and Diprotin A, the numbers of RCSC characterized as $CD34^-/CD45^-/c\text{-}kit^+$ and $CD34^-/CD45^-/Sca1^+$ cells were significantly increased. Again these results were inverted after AMD3100 application. Apparently, our approach enhances the amount of RCSCs specifically by the SDF-1α/CXCR-4 axis. On the one hand, our strategy yields improved cardiac homing of mobilized stem cells which may stimulate RCSC by paracrine means. On the other hand, Tang et al. recently showed that c-kit$^+$ RCSC highly express CXCR4 after hypoxic preconditioning (Tang et al., 2009). Notably, they showed the importance of SDF-1/CXCR4 signaling for RCSC effects on ischemic myocardium which were abolished after in vitro application of AMD3100. These results perfectly match with our findings that RCSC activation by G-CSF and Diprotin A application is dependent on the SDF-1/CXCR-4 axis. These data are important since there is evidence that resident cardiac stem cells play a crucial role for cardiac renewing (Beltrami et al., 2003; Messina et al., 2004). They may stimulate cardiomyocytes via paracrine mechanisms and furthermore may have the potential to differentiate into cardiomyocytes, endothelial or smooth muscle cells in the ischemic heart. However, future studies comprising immunohistological evaluation and cell tracing studies have to analyze these possible effects after dual stem cell therapy in detail.

In summary, our experiments suggest that the beneficial effects of dual stem cell therapy on stem cell homing, cardiac remodeling, heart function and survival are mainly mediated through CXCR4 dependent mechanisms. Therefore, our data strengthen the concept of dual stem cell therapy comprising G-CSF based stem cell mobilization and pharmacological DPP-IV inhibition as a new carrier of hope for treatment after acute myocardial infarction (Theiss et al., 2010).

Materials and methods

Animal model

Animal care and all experimental procedures were performed in strict accordance to the Guide for the Care and Use of Laboratory Animals published by the US National Institutes of Health (NIH publication No. 85-23, revised 1996). C57BL/6 mice were purchased from Charles River (Sulzfeld, Germany). Myocardial infarction (MI) was induced in 8–10 weeks old male C57BL/6 mice by surgical occlusion of the LAD as described previously (Deindl et al., 2006). All experiments concerning survival and cardiac function were performed by the same operator.

Administration of G-CSF, Diprotin A and AMD3100

Experimental design is shown in Supplement 1. Mice were randomly divided into the following groups: Infarcted C57Bl/6 mice (n=20) [AMI] receiving either saline (0.9% NaCl), G-CSF (100 μg/kg/d i.p.) alone [AMI+G-CSF], G-CSF+Diprotin A (70 mg/kg/twice per day) [AMI+G-CSF+DipA], G-CSF+Diprotin A+AMD3100 (1.25 mg/kg/d p.i.) or only AMD3100 [AMI+AMD] for up to 6 days. G-CSF and/or Diprotin A and/or AMD3100 treatment was initiated immediately after the surgical procedure. For analysis of the [AMI], [AMI+G-CSF] and [AMI+G-CSF+DipA] control groups we used data from the animal stocks that have contributed to our previous publication (Zaruba et al., 2009) but also added new animals.

Functional parameter

For evaluation of pressure–volume relationships *in vivo*, mice were anesthetized with thiopental (100 mg/kg, i.p.), intubated and ventilated (MiniVent, HUGO SACHS, Freiburg, Germany). After catheterization via the right carotid artery an impedance-micro manometer catheter (Millar Instruments, Houston, Texas) was introduced into the left ventricle. Raw conductance volumes were corrected for parallel conductance by the hypertonic saline dilution method as described previously (Zaruba et al., 2008). Hemodynamic measurements as well as data analyses were performed by a blinded person using PVAN analysis software (HUGO SACHS, March, Germany).

Histology and immunohistochemistry

At day 30, hearts were excised (n=6 in each group). After fixation in 4% phosphate buffered formalin the hearts were cut transversally into 2 mm thick slices and embedded in paraffin. 4 μm thick sections were cut and mounted on positively charged glass slides. Standard histological procedures (haematoxylin/eosin and Masson trichrome) and immunostaining were executed. Infarct size was determined as area of infarction (AI) correlated to the area of the left ventricle (including LV-septum) in four different slices from the base to the apex of a heart. Total infarct size was calculated by multiplication of the mean percentage value of the circular infarct area with the ratio: vertical extension of the infarct area/total ventricular extension. Measurement of wall thickness was performed by taking the average length of five segments along radii from the center of the left ventricle through the thinnest points of the free LV wall. As analyzed and reported previously, initial infarct sizes are comparable between the different treatment groups as assessed 6 days after myocardial infarction (Zaruba et al., 2009).

For immunostaining, antibodies against CD31 (goat anti-mouse, Santa Cruz) were used. 10 random high-power fields (HPF) from the border zone of each heart sample (n=6) were analyzed concerning the numbers of CD31$^+$ capillaries with 400× magnification as previously described (Zaruba et al., 2009).

Perfusion measurement by single photon emission computed tomography (SPECT)

Imaging was performed 6 and 30 days after LAD ligation as previously described (Wollenweber et al., 2010). Each animal was injected with approximately 370 MBq [99mTc] sestamibi (Covidien, Neustadt/Donau, Germany) in the tail vein. 45 min after injection, the mouse was positioned in the

scanner. We measured left ventricular perfusion using a triple-headed single-photon emission computed tomography system (Prism 3000XP, Philips Medical Systems, Hamburg, Germany). Each detector head was equipped with a 0.5-mm diameter custom-made tungsten knife-edge pinhole collimator (Nuclear Fields, Vortum-Mullem, Holland). The radius of rotation was set to 4 cm (magnification 4-fold), and data were acquired over 60 projection angles (120° for each head), 90 s per projection, giving a total acquisition time of 30 min. Zoom factor was set as 2.0. Center of rotation error was corrected by scanning a multiple point phantom and iteratively adjusting the center-of-rotation offsets. We used the same source to measure the spatial resolution of the system for [99mTc]. Images consisted of a matrix of 128×128×128 with an isotropic voxel size of 0.445 mm. All images were reconstructed using six iterations. Attenuation and scatter correction were not performed in any studies.

Dedicated software was used to generate transverse slices. A volumetric sampling tool was applied to create polar maps of the relative distribution of activity throughout the left ventricle (Nekolla et al., 1998). Each polar map was adjusted for its own maximal value. The size of the defect was calculated with the use of a threshold of 65%, which was derived from the histological infarct sizes. Δ Perfusion was calculated as defect size in % [6 days] − defect size in % [30 days].

Flow cytometry (FACS) of peripheral blood and non-myocyte cardiac cells

8 to 10 weeks old C57BL/6 mice (n=8) were treated with saline, G-CSF, Diprotin A, AMD3100 or combined daily for 6 days. Cells were separated from peripheral blood as described previously (Deindl et al., 2006). The following monoclonal antibodies were used: CD45-PerCP, CD34-FITC, CXCR4-PE (all from BD Pharmingen). Matching isotype antibodies (BD Pharmingen) served as controls. Cells were analyzed by 3-color flow cytometry using a Coulter® Epics® XL-MCLTM flow cytometer (Beckman Coulter). Each analysis included 50,000 events.

Cardiac cells of infarcted hearts of C57BL/6 mice were analyzed 6 days after MI (n=8). Therefore, a myocyte-depleted cardiac cell population was prepared, incubating minced myocardium in 0.1% collagenase IV (Gibco BrL) 45 min at 37 °C, lethal to most adult mouse cardiomyocytes (Zhou et al., 2000). Cells were then filtered through a 70-μm mesh. To exclude spurious effects of enzymatic digestion, BM cells with or without collagenase treatment were stained revealing no significantly changed staining of labeled cell antigens (data not shown). Cells were stained with CD45-PerCP, CD34-FITC, c-kit-PE, CXCR4-PE, Sca1-PE, CD3-biotin, CD45R/B220-biotin, CD11b-biotin, TER-119-biotin, Ly-6G-biotin Abs (all from BD Pharmingen) and subjected to flow cytometry using EPICS XLMCL flow cytometer and Expo32 ADC Xa software (Beckman Coulter). Each analysis included 50,000 events.

Statistical analyses

Results were expressed as mean ± SEM (standard error of mean). Multiple group comparisons were performed by one-way analyses of variance (ANOVA) followed by the Bonferroni procedure for comparison of means. Comparisons between two groups were performed using the unpaired Student's *t*-test. Data were considered statistically significant at a value of $p \leq 0.05$. Analysis of mortality was performed by the Kaplan–Meier-method.

Funding

This work was supported by the German Research Foundation (DFG TH1398/2-1), the Fritz–Bender-Foundation and the Dr. Helmut Legerlotz-Foundation. Markus Vallaster, Christoph Rischpler and Lisa Krieg were funded by the FoeFoLe program of the Ludwig-Maximilians University in Munich.

Conflict of interest

The Ludwig Maximilians University has filed the patents "Use of G-CSF for Treating Ischemia" (EP 03 02 4526.0 and US 60/514,474) and "Remedies for Ischemia" (EP2007/003272 and US 60/792,943).

Acknowledgments

We are grateful to Judith Arcifa, Barbara Markieton and Sandra Junker for their excellent technical assistance. Elements of this study are part of the theses of Markus Vallaster, Christoph Rischpler and Lisa Krieg.

Appendix A. Supplementary data

Supplementary data to this article can be found online at doi:10.1016/j.scr.2011.05.003.

References

Abbott, J.D., Huang, Y., Liu, D., Hickey, R., Krause, D.S., Giordano, F.J., 2004. Stromal cell-derived factor-1alpha plays a critical role in stem cell recruitment to the heart after myocardial infarction but is not sufficient to induce homing in the absence of injury. Circulation 110 (21), 3300–3305.

Aiuti, A., Webb, I.J., Bleul, C., Springer, T., Gutierrez-Ramos, J.C., 1997. The chemokine SDF-1 is a chemoattractant for human CD34+ hematopoietic progenitor cells and provides a new mechanism to explain the mobilization of CD34+ progenitors to peripheral blood. J. Exp. Med. 185 (1), 111–120.

Askari, A.T., Unzek, S., Popovic, Z.B., Goldman, C.K., Forudi, F., Kiedrowski, M., et al., 2003. Effect of stromal-cell-derived factor 1 on stem-cell homing and tissue regeneration in ischaemic cardiomyopathy. Lancet 362 (9385), 697–703.

Balsam, L.B., Wagers, A.J., Christensen, J.L., Kofidis, T., Weissman, I.L., Robbins, R.C., 2004. Haematopoietic stem cells adopt mature haematopoietic fates in ischaemic myocardium. Nature 428 (6983), 668–673.

Beltrami, A.P., Barlucchi, L., Torella, D., Baker, M., Limana, F., Chimenti, S., et al., 2003. Adult cardiac stem cells are multipotent and support myocardial regeneration. Cell 114 (6), 763–776.

Broxmeyer, H.E., Orschell, C.M., Clapp, D.W., Hangoc, G., Cooper, S., Plett, P.A., et al., 2005. Rapid mobilization of murine and human hematopoietic stem and progenitor cells with AMD3100, a CXCR4 antagonist. J. Exp. Med. 201 (8), 1307–1318.

Ceradini, D.J., Kulkarni, A.R., Callaghan, M.J., Tepper, O.M., Bastidas, N., Kleinman, M.E., et al., 2004. Progenitor cell trafficking is regulated by hypoxic gradients through HIF-1 induction of SDF-1. Nat. Med. 10 (8), 858–864.

Christopherson 11, K.W., Hangoc, G., Mantel, C.R., Broxmeyer, H.E., 2004. Modulation of hematopoietic stem cell homing and engraftment by CD26. Science 305 (5686), 1000–1003.

Crump, M.P., Gong, J.H., Loetscher, P., Rajarathnam, K., Amara, A., Arenzana-Seisdedos, F., et al., 1997. Solution structure and basis for functional activity of stromal cell-derived factor-1; dissociation of CXCR4 activation from binding and inhibition of HIV-1. EMBO J. 16 (23), 6996–7007.

Deindl, E., Zaruba, M.M., Brunner, S., Huber, B., Mehl, U., Assmann, G., et al., 2006. G-CSF administration after myocardial infarction in mice attenuates late ischemic cardiomyopathy by enhanced arteriogenesis. FASEB J. 20 (7), 956–958.

Dickstein, K., Cohen-Solal, A., Filippatos, G., McMurray, J.J., Ponikowski, P., Poole-Wilson, P.A., et al., 2008. ESC guidelines for the diagnosis and treatment of acute and chronic heart failure 2008 The Task Force for the Diagnosis and Treatment of Acute and Chronic Heart Failure 2008 of the European Society of Cardiology. Developed in collaboration with the Heart Failure Association of the ESC (HFA) and endorsed by the European Society of Intensive Care Medicine (ESICM). Eur. J. Heart Fail. 10 (10), 933–989.

Engelmann, M.G., Theiss, H.D., Hennig-Theiss, C., Huber, A., Wintersperger, B.J., Werle-Ruedinger, A.E., et al., 2006. Autologous bone marrow stem cell mobilization induced by granulocyte colony-stimulating factor after subacute ST-segment elevation myocardial infarction undergoing late revascularization: final results from the G-CSF-STEMI (Granulocyte Colony-Stimulating Factor ST-Segment Elevation Myocardial Infarction) trial. J. Am. Coll. Cardiol. 48 (8), 1712–1721.

Engelmann, M.G., Theiss, H.D., Theiss, C., Henschel, V., Huber, A., Wintersperger, B.J., et al., 2010. G-CSF in patients suffering from late revascularised ST elevation myocardial infarction: final 1-year-results of the G-CSF-STEMI Trial. Int. J. Cardiol. 144 (3), 399–404.

Fazel, S., Cimini, M., Chen, L., Li, S., Angoulvant, D., Fedak, P., et al., 2006. Cardioprotective c-kit+ cells are from the bone marrow and regulate the myocardial balance of angiogenic cytokines. J. Clin. Invest. 116 (7), 1865–1877.

Franz, W.M., Zaruba, M., Theiss, H., David, R., 2003. Stem-cell homing and tissue regeneration in ischaemic cardiomyopathy. Lancet 362 (9385), 675–676.

Harada, M., Qin, Y., Takano, H., Minamino, T., Zou, Y., Toko, H., et al., 2005. G-CSF prevents cardiac remodeling after myocardial infarction by activating the Jak-Stat pathway in cardiomyocytes. Nat. Med. 11 (3), 305–311.

Huhn, J., Ehrlich, S., Fleischer, B., von Bonin, A., 2000. Molecular analysis of CD26-mediated signal transduction in T cells. Immunol. Lett. 72 (2), 127–132.

Ince, H., Petzsch, M., Kleine, H.D., Eckard, H., Rehders, T., Burska, D., et al., 2005a. Prevention of left ventricular remodeling with granulocyte colony-stimulating factor after acute myocardial infarction: final 1-year results of the Front-Integrated Revascularization and Stem Cell Liberation in Evolving Acute Myocardial Infarction by Granulocyte Colony-Stimulating Factor (FIRSTLINE-AMI) Trial. Circulation 112 (9 Suppl), I73–I80.

Ince, H., Petzsch, M., Kleine, H.D., Schmidt, H., Rehders, T., Korber, T., et al., 2005b. Preservation from left ventricular remodeling by front-integrated revascularization and stem cell liberation in evolving acute myocardial infarction by use of granulocyte-colony-stimulating factor (FIRSTLINE-AMI). Circulation 112 (20), 3097–3106.

Kahne, T., Lendeckel, U., Wrenger, S., Neubert, K., Ansorge, S., Reinhold, D., 1999. Dipeptidyl peptidase IV: a cell surface peptidase involved in regulating T cell growth (review). Int. J. Mol. Med. 4 (1), 3–15.

Messina, E., De Angelis, L., Frati, G., Morrone, S., Chimenti, S., Fiordaliso, F., et al., 2004. Isolation and expansion of adult cardiac stem cells from human and murine heart. Circ. Res. 95 (9), 911–921.

Murry, C.E., Soonpaa, M.H., Reinecke, H., Nakajima, H., Nakajima, H.O., Rubart, M., et al., 2004. Haematopoietic stem cells do not transdifferentiate into cardiac myocytes in myocardial infarcts. Nature 428 (6983), 664–668.

Nekolla, S.G., Miethaner, C., Nguyen, N., Ziegler, S.I., Schwaiger, M., 1998. Reproducibility of polar map generation and assessment of defect severity and extent assessment in myocardial perfusion imaging using positron emission tomography. Eur. J. Nucl. Med. 25 (9), 1313–1321.

Orlic, D., Kajstura, J., Chimenti, S., Limana, F., Jakoniuk, I., Quaini, F., et al., 2001. Mobilized bone marrow cells repair the infarcted heart, improving function and survival. Proc. Natl. Acad. Sci. U.S.A. 98 (18), 10344–10349.

Ruiz, P., Zacharievich, N., Viciana, A.L., Shenkin, M., 1998. Peripheral CD34+ progenitor cells express CD26 and contain increased dipeptidyl peptidase IV activity. Acta Haematol. 100 (2), 110–112.

Saxena, A., Fish, J.E., White, M.D., Yu, S., Smyth, J.W., Shaw, R.M., et al., 2008. Stromal cell-derived factor-1alpha is cardioprotective after myocardial infarction. Circulation 117 (17), 2224–2231.

Segers, V.F., Tokunou, T., Higgins, L.J., MacGillivray, C., Gannon, J., Lee, R.T., 2007. Local delivery of protease-resistant stromal cell derived factor-1 for stem cell recruitment after myocardial infarction. Circulation 116 (15), 1683–1692.

Tang, Y.L., Zhu, W., Cheng, M., Chen, L., Zhang, J., Sun, T., et al., 2009. Hypoxic preconditioning enhances the benefit of cardiac progenitor cell therapy for treatment of myocardial infarction by inducing CXCR4 expression. Circ. Res. 104 (10), 1209–1216.

Theiss, H.D., Brenner, C., Engelmann, M.G., Zaruba, M.M., Huber, B., Henschel, V., et al., 2010. Safety and efficacy of SITAgliptin plus GRanulocyte-colony-stimulating factor in patients suffering from Acute Myocardial Infarction (SITAGRAMI-Trial) — rationale, design and first interim analysis. Int. J. Cardiol. 145 (2), 282–284.

Vanham, G., Kestens, L., De Meester, I., Vingerhoets, J., Penne, G., Vanhoof, G., et al., 1993. Decreased expression of the memory marker CD26 on both CD4+ and CD8+ T lymphocytes of HIV-infected subjects. J. Acquir. Immune Defic. Syndr. 6 (7), 749–757.

Wollenweber, T., Zach, C., Rischpler, C., Fischer, R., Nowak, S., Nekolla, S.G., et al., 2010. Myocardial perfusion imaging is feasible for infarct size quantification in mice using a clinical single-photon emission computed tomography system equipped with pinhole collimators. Mol. Imaging Biol. 12 (4), 427–434.

Zaruba, M.M., Huber, B.C., Brunner, S., Deindl, E., David, R., Fischer, R., et al., 2008. Parathyroid hormone treatment after myocardial infarction promotes cardiac repair by enhanced neovascularization and cell survival. Cardiovasc. Res. 77 (4), 722–731.

Zaruba, M.M., Theiss, H.D., Vallaster, M., Mehl, U., Brunner, S., David, R., et al., 2009. Synergy between CD26/DPP-IV inhibition and G-CSF improves cardiac function after acute myocardial infarction. Cell Stem Cell 4 (4), 313–323.

Zhou, Y.Y., Wang, S.Q., Zhu, W.Z., Chruscinski, A., Kobilka, B.K., Ziman, B., et al., 2000. Culture and adenoviral infection of adult mouse cardiac myocytes: methods for cellular genetic physiology. Am. J. Physiol. Heart Circ. Physiol. 279 (1), H429–H436.

Zohlnhofer, D., Dibra, A., Koppara, T., de Waha, A., Ripa, R.S., Kastrup, J., et al., 2008. Stem cell mobilization by granulocyte colony-stimulating factor for myocardial recovery after acute myocardial infarction: a meta-analysis. J. Am. Coll. Cardiol. 51 (15), 1429–1437.